

Transient amplification in Floquet media: the Mathieu oscillator example

Ioannis Kiropelidis,^{1,2} Fotios K. Diakonou,² Georgios Theocharis,¹ and Vincent Pagneux¹

¹*LAUM, UMR-CNRS 6613, Le Mans Université, Av. O. Messiaen, 72085, Le Mans, France*

²*Department of Physics, University of Athens, 15784, Athens, Greece*

The Mathieu equation occurs naturally in the description of non linear vibrations or by considering the propagation of a wave in an infinite medium with time-periodic refractive index. It is known to lead to parametric instability since it supports unstable solutions in some regions of the parameter space. However, even in the stable region the matrix that propagates the initial conditions forward in time is non-normal and therefore it can result in transient amplification. By optimizing over initial conditions as well as initial time we show that significant transient amplifications can be obtained, going beyond the one simply stemming from adiabatic invariance. Moreover, we explore the monodromy matrix in more depth, by studying its ϵ -pseudospectra and Petermann factors, demonstrating that is the degree of non-normality of this matrix that determines the global amplifying features.

I. INTRODUCTION

Over the last years, the modulation of the properties of materials in time has attracted great interest [1–3]. Time-varying metamaterials exhibit rich phenomenology, ranging from time-reflection and time-refraction [4] to non-trivial topological features [5]. When these modulations are periodic in time, the prism of Floquet analysis can be used, leading to the development of Floquet metamaterials [6, 7]. Meanwhile, Floquet theory captures the stability properties of the solutions in terms of the Floquet exponents and is known that unstable solutions are related with parametric resonances. These are appearing in a wide range of time-varying systems as for instance in photonic time crystals [8] and in elastic metamaterials [9, 10].

Amplification in time varying media is closely related with the concept of parametric instability, but there are other ways to amplify a system as well. For example, a new mechanism for gain was recently found in time-dependent photonic metamaterials [11], resulting from the compression of the lines of the electric and magnetic fields. Furthermore, it is known, especially in hydrodynamics [12, 13], that stable solutions of a system can be transiently amplified when the matrix that propagates the initial conditions forward in time is non-normal, having thus non orthogonal eigenvectors [14, 15]. Along this line, the pseudospectrum tool was developed in order to describe these transient amplifying phenomena [16]. Let us remark that non-normality and pseudospectrum appear to play an important role in the emerging field of non-Hermitian topology, either for time-transient [17, 18] or non-Hermitian skin effect spectrum [18–20].

Following the previous considerations, a prototype equation that: (i) is of particular interest in the context of wave propagation in time varying media [21, 22] and (ii) has been reported to possess stable solutions that can be transiently amplified [23], is the venerable Mathieu equation [24]. It is among the well studied equations in physics and up to this day has been found to govern the dynamics of many systems [25]. Typical examples are

an inverted pendulum whose pivot point vibrates vertically [26], a charged particle in a Paul trap [27], a liquid layer that is vertically oscillated [28], etc. Properties of the Mathieu equation have been investigated in numerous classical textbooks [29–32] and it is known that both stable and unstable solutions are supported [33, 34]. Several experiments have demonstrated the possibility of parametric amplification in platforms that are described by the Mathieu equation, see for instance ref. [35] and the references within. It has been shown that stable solutions of the Mathieu equation are good candidates to be transiently amplified because the matrix that propagates the initial conditions forward in time is non-normal [23], yet, open questions remain.

In this paper we make a comprehensive investigation of the transient amplification exhibited by a wave that propagates in an infinite harmonically modulated medium. We consider wave dynamics governed by the Mathieu equation and we explore in detail the transient amplification of its stable solutions. By appropriate change of variables, we focus on growths supplementary to evident adiabatic invariance. Owing to the ϵ -pseudospectrum of the monodromy matrix – the matrix that propagates the initial conditions over one period – we reveal that the initial time t_0 has a strong impact to the maximum transient amplification. In addition, we provide numerical evidence that the global maximum amplification is captured merely by the monodromy matrix.

Our work is organized as follows: In Section II we consider the propagation of a wave in an infinite one-dimensional medium that is periodically modulated in time, so that the Mathieu equation emerges. In Section III we briefly remind the basic properties of the Mathieu equation and we derive its stability chart. In Section IV we give a few examples of stable solutions that are transiently amplified and we introduce a measure for the quantification of the transient amplification that filters the one that stems from adiabatic invariance. In Section V we explore the impact of the initial time in these amplifying features and we explain the underlying physics in terms of the non-normality of the monodromy matrix, while in Section VI we calculate the overall maxi-

num amplification of the stable solutions of the Mathieu equation. Then, in Section VII we present the evolution of a wave that propagates in a Mathieu medium and experiences the biggest possible transient amplification. Finally, in Section VIII we summarize our findings.

II. WAVE PROPAGATION IN A TIME-VARYING MEDIUM

We follow ref. [22] and we study wave propagation in an infinite harmonically modulated medium that is governed by the following wave equation

$$\frac{\partial^2 \psi(x, \tau)}{\partial \tau^2} = \left[\tilde{\delta} - 2\tilde{q} \cos(\Omega\tau) \right] \frac{\partial^2 \psi(x, \tau)}{\partial x^2} \quad (1)$$

where $\tilde{\delta}$, \tilde{q} and Ω are constants. Such a wave equation describes the propagation of an electromagnetic wave in a medium with electric permittivity $\epsilon(t) = \epsilon_0 / [\tilde{\delta} - 2\tilde{q} \cos(\Omega\tau)]$ (the speed of light is $c = 1$ and ϵ_0 is the vacuum permittivity) [21]. It could also correspond to the propagation of an elastic wave in a medium with time-dependent stiffness [9]. By separation of variables, one class of solutions of Eq. (1) are $\psi(x, \tau) = f(\tau)h(x)$ and by substituting this form into Eq. (1) we arrive at the following set of ODE's that f and h satisfy

$$\frac{d^2 h(x)}{dx^2} + k^2 h(x) = 0 \quad (2)$$

$$\frac{d^2 f(\tau)}{d\tau^2} + k^2 \left[\tilde{\delta} - 2\tilde{q} \cos(\Omega\tau) \right] f(\tau) = 0 \quad (3)$$

where k is the real wave number of the wave. From Eq. (2) we get that $h(x)$ has the form $h(x) \sim e^{\pm ikx}$, while Eq. (3) after time rescaling $t = \Omega\tau/2$ and setting $\delta = 4k^2\tilde{\delta}/\Omega^2$, $q = 4k^2\tilde{q}/\Omega^2$ drops to the usual form of the Mathieu equation, that is

$$\ddot{f} + \omega^2(t)f = 0 \quad (4)$$

with $\omega^2(t) = \delta - 2q \cos(2t)$. Notice that dot represents differentiation with respect to the time t . The Mathieu equation contains both stable and unstable – exponentially growing – solutions, according to the values of the parameters (δ, q) . The amplification is usually related with the exponentially growing solutions, namely with the parametric instability. However, a wave can experience amplification even with asymptotic stability [16]. In this case the amplification is a transient phenomenon characterizing the stable solutions of the Mathieu equation. We will perform a detailed analysis of this transient amplification employing suitable tools for its quantitative description. Before proceeding to this analysis we give a brief review of Mathieu equation.

III. REVIEW OF MATHIEU EQUATION

The Mathieu equation written as a system of two linear first order differential equations gets the form

$$\dot{\boldsymbol{\eta}}(t) = \mathbf{A}(t)\boldsymbol{\eta}(t), \quad (5)$$

with $\boldsymbol{\eta}(t) = \begin{pmatrix} f(t) \\ \dot{f}(t) \end{pmatrix}$ and $\mathbf{A}(t) = \begin{pmatrix} 0 & 1 \\ -\omega^2(t) & 0 \end{pmatrix}$. The general solution of Eq. (5) can be written in the form

$$\boldsymbol{\eta}(t) = \boldsymbol{\Psi}(t, t_0)\boldsymbol{\eta}(t_0), \quad (6)$$

with initial condition $\boldsymbol{\eta}(t_0)$. The matrix $\boldsymbol{\Psi}(t, t_0)$ which evolves the initial vector in time, will be called the principal matrix solution [33].

The matrix $\mathbf{A}(t)$ that contains the parameters of the Mathieu equation is π periodic, i.e., $\mathbf{A}(t) = \mathbf{A}(t + \pi)$. Therefore, Floquet theory applies and states that the stability properties of the solutions can be deduced by the eigenvalues of the matrix $\boldsymbol{\Psi}(t_0 + \pi, t_0)$, termed the monodromy matrix. These eigenvalues, which we denote as λ_{\pm} and which are commonly called Floquet multipliers, do not depend on the choice of the initial time t_0 since two matrices $\boldsymbol{\Psi}(\pi + t_1, t_1)$ and $\boldsymbol{\Psi}(\pi + t_2, t_2)$ are similar [33].

From Liouville's formula, $\det[\boldsymbol{\Psi}(t_0 + \pi, t_0)] = \exp\left[\int_{t_0}^{t_0+\pi} \text{Tr}\mathbf{A}(s)ds\right]$, it follows that the determinant of the monodromy matrix $\boldsymbol{\Psi}(t_0 + \pi, t_0)$ is 1 and therefore its two eigenvalues λ_{\pm} satisfy the relation $\lambda_+ \lambda_- = 1$. When $|\lambda_{\pm}| = 1$, they are complex conjugates and are restricted to lie in the unit circle in the complex plane: the solutions are stable. When $|\lambda_{\pm}| \neq 1$ the typical solutions are unstable and grow exponentially with time. Figure 1(a) illustrates the norm of these eigenvalues for each pair of the only parameters of equation (4) (δ and q). The gray region of this chart (apart from the boundaries)

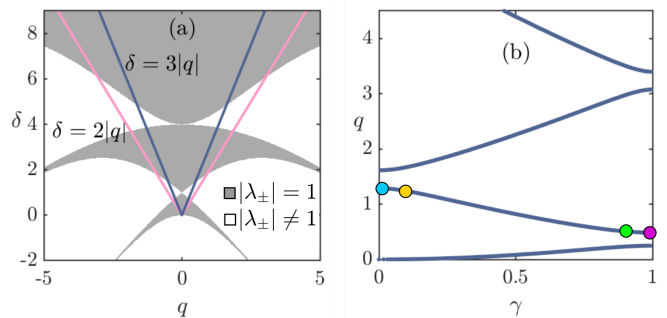


FIG. 1. Stability diagrams of Mathieu equation (4). (a) Shown here is the norm of the eigenvalues λ_{\pm} of the monodromy matrix as a function of the parameters δ and q . Stable regions are in grey color. Also shown are two cuts of the form $\delta = c|q|$ with $c = 2, 3$. (b) Floquet exponent γ as the line $\delta = 3|q|$ is scanned. The circles correspond to the four cases that will be displayed in Fig. 2.

corresponds to stable solutions, while in the white region $|\lambda_{\pm}| \neq 1$. The boundary between these two regions corresponds to exceptional points where the typical solutions grow linearly with time. This plot is widely known as the stability chart of the Mathieu equation [24].

The stability properties of periodic systems are usually studied in terms of the Floquet exponent γ , which is related with the Floquet multipliers by $\lambda_{\pm} = e^{\pm i\gamma\pi}$. In Fig. 1(b) we present the exponent γ along the cut $\delta = 3q$ (δ/q is constant for constant $\tilde{\delta}$, \tilde{q} and Ω). This is a Floquet spectrum, with the bands corresponding to the stable regions and the gaps to the unstable ones [36].

IV. TRANSIENT AMPLIFICATION

In this section and in the remaining of this work, we will elaborate on the transient amplification that is displayed by the stable solutions of the Mathieu equation (Fig. 1). To illustrate this, in Fig. 2(a)-(d) we plot $f(t)$ and $\dot{f}(t)$ for the four cases that are shown in Fig. 1(b). In Fig. 2(a) and (b) the initial conditions are $f(0) = 1$ and $\dot{f}(0) = 0$ while in Fig. 2(c) and (d) the corresponding initial conditions are $f(0) = 0$ and $\dot{f}(0) = 1$. Notice that in all cases the closer to the edges of the bands, the stronger the amplification is. This transient amplification cannot be captured by the stability analysis since the Floquet exponents are purely imaginary in all these examples. It is due to the non-normality of the principal matrix $\Psi(t, t_0)$ [16, 37].

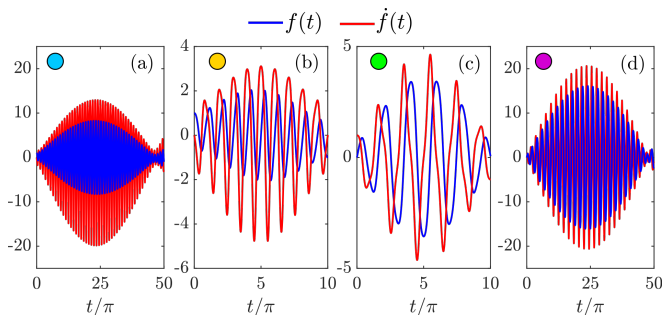


FIG. 2. Typical solutions of Mathieu equation (4) in the stable regime. In all cases the sets of parameters (δ, q) lie in the line $\delta = 3q$. (a) Evolution of the initial conditions $f(0) = 1$ and $\dot{f}(0) = 0$ when $q = 1.285 / \gamma = 0.02$. This set of parameters is indicated with the blue circle in Fig. 1(b). (b) Same as (a) but $q = 1.239 / \gamma = 0.1$ - yellow circle in Fig. 1(b). (c) Same as (a) but $q = 0.507 / \gamma = 0.9$ - green circle in Fig. 1(b). Also the initial conditions are $f(0) = 0$ and $\dot{f}(0) = 1$ in this case. (d) Same as (c) but $q = 0.4855 / \gamma = 0.98$ - purple circle in Fig. 1(b).

A. Choice of variables

We choose to change variables to the following ones

$$X = f\sqrt{\omega(t)} \quad , \quad Y = \dot{f}/\sqrt{\omega(t)}. \quad (7)$$

To illuminate the utility of this transformation one should consider the WKB limit of Eq. (4), that is when $\omega(t)$ varies slowly with time, i.e., $\Omega \ll \omega$. We can show then that in the WKB limit the norm of the vector $\xi(t) = \begin{pmatrix} X(t) \\ Y(t) \end{pmatrix}$, i.e., $\|\xi(t)\| = \sqrt{|X(t)|^2 + |Y(t)|^2}$, is constant and equal to $\sqrt{|X(0)|^2 + |Y(0)|^2}$ (it is the adiabatic invariant of Eq. (4) [38]). This WKB adiabatic invariant is already predicting amplification with the WKB solution given by $f(t) = e^{\pm i \int_0^t \omega(s) ds} / \sqrt{\omega(t)}$, but in this paper we will try to go beyond this adiabatic effect and we filter this by choosing these new variables [39]. Away from the WKB limit the norm of the vector $\xi(t)$ is not constant: non-trivial amplification is captured, non-trivial in the sense that it is not predicted by WKB. In Appendix A we present some examples showing the convergence to WKB limit for large parameters δ and q .

Using Eq. (5) and Eq. (7), we get that

$$\dot{\xi}(t) = \mathbf{C}(t)\xi(t), \quad (8)$$

where $\mathbf{C}(t)$ is the π -periodic matrix $\begin{pmatrix} \dot{\omega}/2\omega & \omega \\ -\omega & -\dot{\omega}/2\omega \end{pmatrix}$.

Moreover, the vector $\xi(t)$ is given in terms of the initial state vector $\xi(t_0)$ as

$$\xi(t) = \Phi(t, t_0)\xi(t_0), \quad (9)$$

where the matrix $\Phi(t, t_0)$ is expressed in terms of the principal matrix $\Psi(t, t_0)$ through the relation

$$\Phi(t, t_0) = \begin{pmatrix} \frac{\sqrt{\omega(t)}}{\sqrt{\omega(t_0)}} \Psi_{11}(t, t_0) & \sqrt{\omega(t)\omega(t_0)} \Psi_{12}(t, t_0) \\ \frac{1}{\sqrt{\omega(t)\omega(t_0)}} \Psi_{21}(t, t_0) & \frac{\sqrt{\omega(t_0)}}{\sqrt{\omega(t)}} \Psi_{22}(t, t_0) \end{pmatrix}. \quad (10)$$

Since $\omega(t_0 + \pi) = \omega(t_0)$ the monodromy matrices $\Phi(t_0 + \pi, t_0)$ and $\Psi(t_0 + \pi, t_0)$ share the same eigenvalues, namely the Floquet multipliers λ_{\pm} .

B. Choice of measure

As we noted before, to avoid amplification simply obtained by adiabatic invariance, it is the norm of $\xi(t)$ that we will use as a measure for the amplification. In particular, the maximum possible amplification is given by the maximum of the norm of $\xi(t)$ at a given t over all the initial conditions $\xi(t_0)$ at a given t_0 . This is equivalent with the 2-norm of the matrix $\Phi(t, t_0)$ since by definition this matrix norm is given by

$$\|\Phi(t, t_0)\| = \max_{\xi(t_0), \|\xi(t_0)\|=1} \|\Phi(t, t_0)\xi(t_0)\|. \quad (11)$$

Therefore, the quantity $\|\Phi(t, t_0)\|$ reveals the maximum possible amplification of the vector $\xi(t)$ at time t , out of all the initial conditions at t_0 .

The norm of $\Phi(t, t_0)$ and the corresponding maximizing initial condition $\xi(t_0)$ are provided by the singular value decomposition (SVD) [40]. The SVD of a real matrix is the decomposition $\Phi(t, t_0) = \mathbf{U}(t, t_0)\mathbf{\Sigma}(t, t_0)\mathbf{V}^T(t, t_0)$, where $\mathbf{\Sigma}(t, t_0)$ is a diagonal matrix with real and nonnegative entries that are arranged in descending order. Also, $\mathbf{U}(t, t_0)$ and $\mathbf{V}(t, t_0)$ are orthogonal matrices and T denotes the transpose. The largest singular value $\sigma_{max}(t, t_0)$ (that is the first element of $\mathbf{\Sigma}(t, t_0)$) is the norm $\|\Phi(t, t_0)\|$. Furthermore, the SVD provides also the most amplified initial condition $\xi(t_0)$: the first column of the matrix $\mathbf{V}(t, t_0)$.

Figure 3(a) illustrates the norm of the propagator $\Phi(t, 0)$ as a function of the time t , for the set of parameters (δ, q) that is used in Fig. 2(c). The norm clearly exceeds 1, showing the existence of transient amplification in the stable regime. Moreover, the norm of the propagator is periodic when the exponent $\gamma = m_1/m_2$ and is of period at most $m_2\pi$ [29]. Therefore, in this example where $\gamma = 0.9$, the norm of the propagator oscillates with a period of 10π . Besides, the norm of $\Phi(t, 0)$ at time $t = 5.32\pi$ is the maximum possible amplification that we can get for this set of parameters with $t_0 = 0$. In Fig. 3(b) and (c) we present the evolution with time of the variables X and Y when 2 different initial conditions are considered. Both of these initial conditions yield the maximum value of $\|\xi(t)\|$, but at 2 different "final" time t , at $t = 0.8\pi$ in (b) and at $t = 5.32\pi$ in (c). We present in Fig. 3(b) and (c) the corresponding norms of ξ . Also shown are the quantities $\pm\sqrt{|X(0)|^2 + |Y(0)|^2} = \pm 1$ (adiabatic prediction) in order to clearly see the non-trivial amplification non predicted by simple adiabatic invariance. We note here that similar transient amplifying phenomena occur for other time-dependent systems as well (see Appendix B for the Meissner equation – piecewise constant frequency $\omega(t)$).

C. Floquet representation and pseudospectrum

In this part, to describe the amplification the focus will be put on the monodromy matrix. The Floquet theory states that the propagator $\Phi(t, t_0)$ is written in the form [33]

$$\Phi(t, t_0) = \mathbf{P}(t, t_0)e^{\mathbf{B}(t_0)(t-t_0)}, \quad (12)$$

where the matrix $\mathbf{P}(t, t_0)$ is π -periodic on both times t and t_0 while the matrix $\mathbf{B}(t_0)$ depends only on the initial time t_0 . The monodromy matrix will be denoted by $\mathbf{M}(t_0)$ as

$$\mathbf{M}(t_0) = e^{\mathbf{B}(t_0)\pi}. \quad (13)$$

Iterated powers $\|\mathbf{M}^n(t_0)\|$ equal to $\|\Phi(t_0 + n\pi, t_0)\|$ provide the maximum possible amplification at each multiple

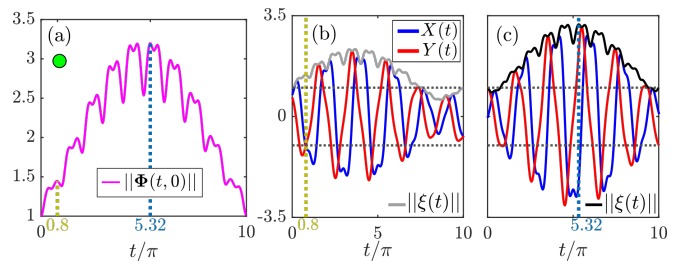


FIG. 3. Evolution of the norm of the propagator. The set of parameters (δ, q) that is used in this figure is the one that is also used in Fig. 2(c), namely $q = 0.507$ and $\delta = 3q$, which result in a Floquet exponent $\gamma = 0.9$. (a) Shown here is the norm of the propagator matrix $\Phi(t, 0)$. (b) Evolution of the initial conditions $X(0) = 0.7469$ and $Y(0) = 0.6649$ which yield the maximum norm of the vector $\xi(t)$ at time $t = 0.8\pi$. The solid curve is the norm of $\xi(t)$. (c) Same as (b) with initial conditions $X(0) = -0.0449$ and $Y(0) = 0.999$ which yield the maximum norm of the vector $\xi(t)$ at time $t = 5.32\pi$. Also shown with black solid curve is the norm of $\xi(t)$. In (b) and (c), the dotted lines represent the quantities $\pm\sqrt{|X(0)|^2 + |Y(0)|^2} = \pm 1$.

of π and a stroboscopic view of the amplification. It is illustrated in Fig. 4(a) where we present $\|\mathbf{M}^n(0)\|$ and the associated norm of the propagator $\|\Phi(t, 0)\|$ for the same set of parameters as in Fig. 3. We already see that this stroboscopic point of view gives useful hints on the amplification. We now concentrate on finding lower bound for $\max_n \|\mathbf{M}^n(t_0)\|$ using the concept of pseudospectrum.

The ϵ -pseudospectrum [16] of the matrix $\mathbf{M}(t_0)$ is defined as the set of all the complex numbers z such that

$$\|(z - \mathbf{M}(t_0))^{-1}\| > \epsilon^{-1}, \quad (14)$$

with $\epsilon > 0$. Note that the eigenvalues are points corresponding to $\epsilon \rightarrow 0$. In Fig. 4(b) are shown the boundaries of the ϵ -pseudospectrum of $\mathbf{M}(0)$ for different values of ϵ where the eigenvalues of $\mathbf{M}(0)$ appear as singularities; the behavior of the pseudospectrum around these singularities gives directly lower bound for amplification. Indeed, the pseudospectrum provides several useful bounds. For instance, the maximum value of $\|\mathbf{M}^n(t_0)\|$ can be estimated by

$$\max_n \|\mathbf{M}^n(t_0)\| \geq \max_{\epsilon} \frac{\rho_{\epsilon}(\mathbf{M}(t_0)) - 1}{\epsilon} \quad (15)$$

where $\rho_{\epsilon}(\mathbf{M}(t_0))$ is the so called ϵ -pseudospectrum radius, given by

$$\rho_{\epsilon}(\mathbf{M}(t_0)) = \max \{ |z| : z \in \mathbb{C}, \|(z - \mathbf{M}(t_0))^{-1}\| > \epsilon^{-1} \}. \quad (16)$$

The quantity at the r.h.s of Eq. (15) is the Kreiss constant [41]. If the Kreiss constant is more than 1, then non trivial amplification is captured. At the inset of Fig. 4(b) we present the quantity $[\rho_{\epsilon}(\mathbf{M}(0)) - 1]/\epsilon$ as a function

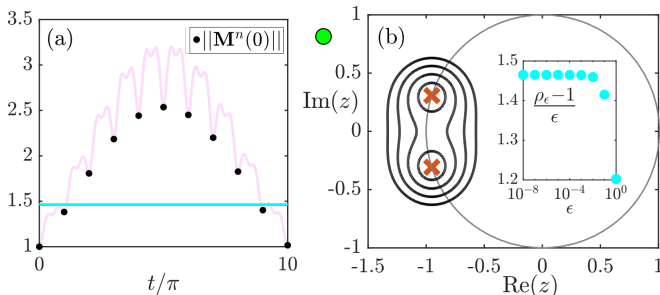


FIG. 4. Amplification in terms of the monodromy matrix and its ϵ -pseudospectrum. We use the same set of parameters (δ, q) as in Fig. 3. (a) The black dots denote the quantity $\|\mathbf{M}^n(0)\|$ and the magenta line the norm $\|\Phi(t, 0)\|$. The cyan line corresponds to the Kreiss constant which provides a bound for $\max_n \|\mathbf{M}^n(0)\|$. (b) With crosses are shown the eigenvalues of $\mathbf{M}(0)$ which lie in the unit circle (shown with solid gray line). The black solid lines are the boundaries of the ϵ -pseudospectrum for $\epsilon = 0.08, 0.14, 0.2, 0.26$. In the inset is shown the quantity at the right hand side in Eq. (15) which is a bound for the amplification. The shown plateau corresponds to the Kreiss constant, displayed also in (a) with the cyan line.

of ϵ . The plateau that is shown determines the Kreiss constant which exceeds 1 indicating amplification (see also Fig. 4(a)).

V. IMPACT OF THE INITIAL TIME

Until now, t_0 was assumed to be zero. A priori, there is no reason that it is giving the best amplification; thus we are now going to investigate other values of the initial time. At the top three panels in Fig. 5(a)-(c) we show the norm $\|\Phi(t, t_0)\|$ as a function of t for three different choices of t_0 . At the same panels we also show the stroboscopic monodromy norm $\|\mathbf{M}^n(t_0)\|$ as a function of n . These panels indicate that the initial time t_0 has an influence that should be taken into account. Going into the evaluation of the amplification lower bound we face an interesting situation: varying t_0 the pseudospectrum of $\mathbf{M}(t_0)$ is evolving but its eigenvalues are pinned at fixed positions (due to the similarity of two matrices $\mathbf{M}(t_1)$ and $\mathbf{M}(t_2)$ - see Section III). This is illustrated in Fig. 5 (bottom panels), where is reported the evolution of the pseudospectrum (as well as the non-normality) of $\mathbf{M}(t_0)$. This evolution with t_0 is also reflected by the change of the lower bound given by the Kreiss constant.

A closer look in Fig. 5 reveals that for $t_0 = 0.32\pi$, the maximum amplification is provided merely by the monodromy matrix. This observation drive us to investigate whether something special happens for this particular initial time. To that end, in Fig. 6(a) we illustrate the quantities $\max_t \|\Phi(t, t_0)\|$ [42] and $\max_n \|\mathbf{M}^n(t_0)\|$ as a function of t_0 and we observe that their maxima coincide for $t_0 = 0.32\pi$. The overall maximum ampli-

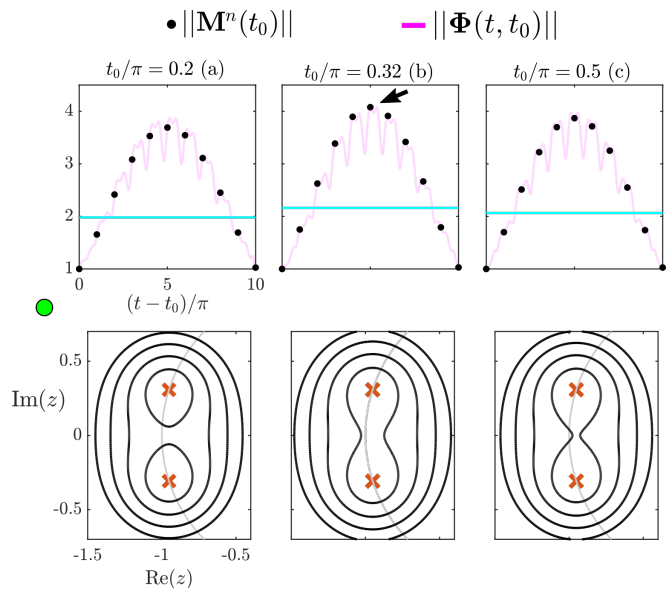


FIG. 5. Influence of the initial time t_0 . In all cases we use the same set of parameters (δ, q) as in Fig. 3. Top figures (a)-(c): Shown here are the quantities $\|\Phi(t, t_0)\|$ as a function of t (magenta lines) and $\|\mathbf{M}^n(t_0)\|$ as a function of $n = 0, 1, \dots, 10$ (black dots), for three initial times (a) $t_0 = 0.2$. (b) $t_0 = 0.32$. (c) $t_0 = 0.5$. Also shown with cyan lines are the Kreiss constants. Bottom figures (a)-(c): Corresponding boundaries of the pseudospectra for $\epsilon = 0.08, 0.14, 0.2$ and 0.26 . Also shown with crosses are the Floquet multipliers which lie in the unit circle and do not change as t_0 changes.

fication is captured merely by the monodromy matrix. More insight into this last result is provided by studying the Kreiss constant for all t_0 . It displays the same pattern as previously with its maximum for $t_0 = 0.32\pi$ (see Fig. 6(b)).

Another measure that examines non-normality of a matrix is its Petermann factors [16, 43, 44] (or conditioning number). The two Petermann factors of the monodromy matrix are given by

$$K_{\pm} = \frac{\|u_{\pm}\| \|v_{\pm}\|}{|v_{\pm}^{\dagger} u_{\pm}|}, \quad (17)$$

where $\mathbf{u}_{\pm}(t_0)$, $\mathbf{v}_{\pm}(t_0)$ correspond respectively to right and left eigenvectors associated to eigenvalues λ_{\pm} . For a normal matrix the Petermann factors are equal to 1. In the case of the monodromy matrix in our problem its two Petermann factors K_{\pm} are equal because its eigenvalues are complex conjugates in the stable region and therefore the two right and left eigenvectors are also complex conjugates, namely $\mathbf{u}_{+} = \bar{\mathbf{u}}_{-}$ and $\mathbf{v}_{+} = \bar{\mathbf{v}}_{-}$. In Fig. 6(c) we present the Petermann factor $K = K_{+} = K_{-}$ of the monodromy matrix as a function of the initial time, for the same set of parameters δ and q used in Fig. 6(a), (b). It confirms that non-normality is maximum for $t_0 = 0.32\pi$.

From the analysis of this part, it appears that the monodromy matrix is capable to determine the overall maxi-

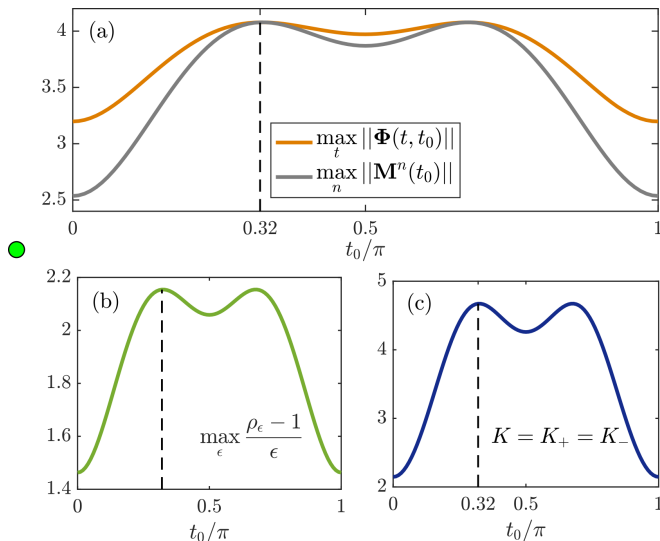


FIG. 6. Evolution with t_0 of the nonnormality of the propagator. We use the same set of parameters (δ, q) as in Fig. 3. (a) Shown here is the $\max_t \|\Phi(t, t_0)\|$ and the quantity $\max_n \|\mathbf{M}^n(t_0)\|$ where n is an integer number. (b) Kreiss constant, i.e., $\max_\epsilon \{[\rho_\epsilon(\mathbf{M}(t_0)) - 1]/\epsilon\}$ as a function of the initial time t_0 . (c) Shown here are the Petermann factors $K = K_+ = K_-$ of the monodromy matrix as the initial time t_0 changes. The Petermann factors measure the parallelism of its right and left eigenvectors.

mum amplification for the Mathieu equation. This latter occurs when the non-normality of the monodromy matrix is maximal. This property seems to be general as verified through numerical investigations for a dense set of parameters δ and q .

VI. MAXIMUM TRANSIENT AMPLIFICATION: MONODROMY MATRIX DESCRIPTION

The goal of this part is to calculate the maximum possible amplification of all the stable solutions. In this section we study the quantity

$$\max_{t_0} \left[\max_t \|\Phi(t, t_0)\| \right], \quad (18)$$

at the stable region of the stability chart [45]. Figure 7(a) displays the global maximum (Eq. (18)) in the parameter plane (δ, q) . Note that we consider exclusively the case of positive ω^2 or positive permittivity, restricting our analysis within the parameter domain inside the cone $\delta = 2|q|$. It is clear that the solutions close to the unstable region are intensively amplified. In fact, this maximum amplification diverges as the boundary with the unstable region is approached. Obviously along the line $\delta = 0$ no amplification is captured, since the Mathieu equation drops to the equation of the harmonic oscillator. The comparison with the stroboscopic monodromy norm is dis-

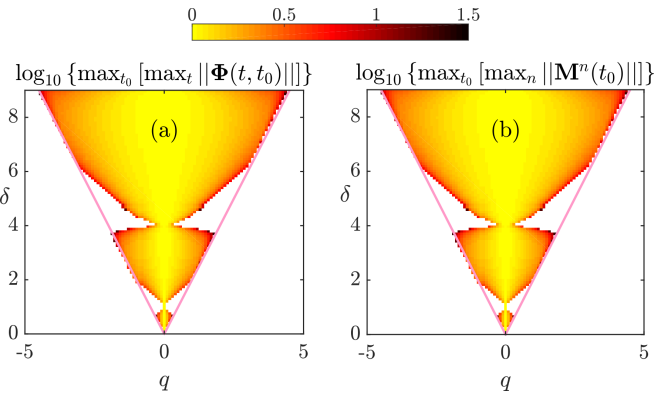


FIG. 7. Global maximum amplification over all initial conditions and all initial times. (a) Shown here is the quantity $\log_{10} \{\max_{t_0} [\max_t \|\Phi(t, t_0)\|]\}$ and (b) $\log_{10} \{\max_{t_0} [\max_n \|\mathbf{M}^n(t_0)\|]\}$. These quantities are calculated at the stable regime inside the cone that is formed by the line $\delta = 2|q|$.

played in Fig. 7(b) with $\max_{t_0} [\max_n \|\mathbf{M}^n(t_0)\|]$. Comparing Fig. 7(a) and (b) confirms that the monodromy matrix is able to predict the amplification. These results support our conjecture that the monodromy matrix determines the overall maximum amplification exhibited by the stable solutions of the Mathieu equation.

VII. BACK TO THE WAVE PROPAGATION

In this last section we give an example of wave evolution governed by Eq. (1). The solution is given by $\psi(x, t) = h(x)f(t)$ with $h(x) = e^{ikx}$ and f is a solution of Mathieu equation (4). We use the same set of parameters (δ, q) and t_0 as in Fig. 5(b); this t_0 resulting in the maximization of the chosen norm.

In Fig. 8(a) we present the real part of the solution $\psi(x, t)$ with initial conditions given by SVD providing the best amplification for $t = 5.32\pi$ and $t_0 = 0.32\pi$. The result is a standing wave that is transiently amplified in time. If, instead, we simply take initial conditions that correspond to one Floquet mode (one eigenvector of the monodromy matrix) transient amplification is suppressed (Fig. 8(b)).

VIII. CONCLUSIONS AND DISCUSSION

We have shown that a standing wave in an infinite medium that is periodically modulated in time, experiences transient amplification even with asymptotic stability. To explore this effect, we studied the transient amplifying features of the stable solutions of the Mathieu equation, which are known to be due to the non-normality of the propagator matrix. We applied several methods (the ϵ -pseudospectrum, the Kreiss constant etc)

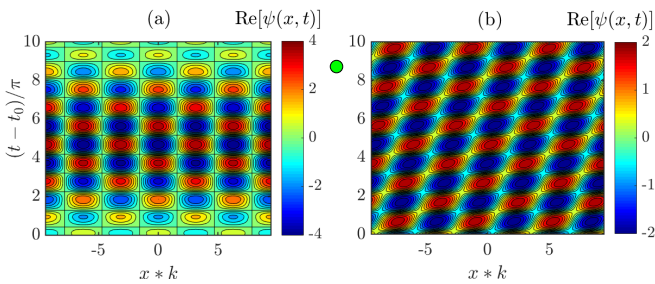


FIG. 8. Space-time evolution of $\psi(x, t)$ satisfying Eq. (1). (a) We use as initial conditions the ones that the SVD yields and which result in the maximization of the norm that we have chosen. (b) We project the initial conditions that the SVD yields in the two Floquet modes and we cancel the contribution from one of these Floquet modes.

classically used in problems of non-normal nature. Moreover, we have taken into account the impact of the initial time and we have shown that the monodromy matrix produces the overall maximum transient amplification.

Our work has led to many questions which could be the basis of new studies. First of all, the addition of a loss factor would be of importance in view of experimental realization; then, it is expected that even with asymptotic decay a wave could still experience transient amplification for small times. Furthermore, it would be of interest to investigate the possible transient amplification experienced by a wave that is scattered through a slab with time-varying permittivity.

IX. ACKNOWLEDGEMENTS

The authors would like to thank N. Bakas and P. J. Ioannou for fruitful discussions. I. K. acknowledges financial support from the Institute d'Acoustique - Graduate School of Le Mans and from the Academy of Athens.

Appendix A: Norm of the vector ξ

We present in Fig. 9 the norm of the vector $\xi(t)$ for four different sets (δ, q) . In all cases, the parameters lie in the line $\delta = 3q$, the exponent γ is approximately equal to 0.5 and the initial conditions are $X(0) = Y(0) = 1/\sqrt{2}$. As the parameters of the Mathieu equation increase, the norm of the vector ξ tends to the constant value $\sqrt{X^2(0) + Y^2(0)} = 1$.

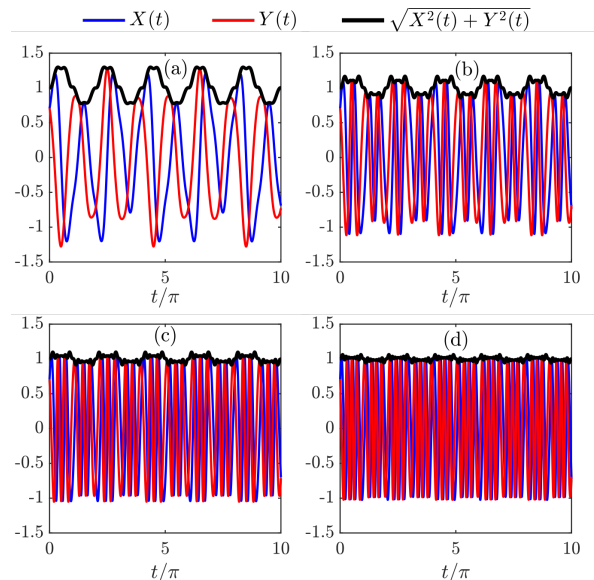


FIG. 9. Shown are the variables $X(t)$ and $Y(t)$ as well as the quantity $\sqrt{|X(t)|^2 + |Y(t)|^2}$ as a function of time. In all cases $\delta = 3q$ and in (a) $q = 0.82$, (b) $q = 4.4$, (c) $q = 10.79$ and (d) $q = 20.03$. All these choices result in an exponent γ that is approximately equal to 0.5.

Appendix B: Meissner equation

We consider here the case of a harmonic oscillator with piecewise constant time-dependent frequency $\omega(t)$ (Meissner equation [36]), i.e. $\ddot{f} + \omega^2(t)f = 0$, varying periodically between the values $\omega_1 = \sqrt{\kappa_1 - 2\kappa_2}$ and $\omega_2 = \sqrt{\kappa_1 + 2\kappa_2}$ with $\kappa_{1,2}$ constants (see Fig. 10(a)). The parameter $\delta\tau$ in Fig. 10(a) controls the time intervals $\Delta t_{1,2}$ spend in the frequency values $\omega_{1,2}$, where $\Delta t_{1,2} = \pi/2 \pm \delta\tau$. When $\delta\tau \neq 0$, the symmetry $\kappa_2 \rightarrow -\kappa_2$ is broken, leading to a deformation in the shape of the stability chart. This is shown in Fig. 10(b) and (c) where two different values of $\delta\tau$ are chosen, $\delta\tau = 0$ in (b) and $\delta\tau = 4\pi/29$ in (c).

In order to quantify the amplification of the stable solutions, following the same transformation as in Eq. (7), we find that the monodromy matrix

$$\Phi(\pi, 0) = \begin{pmatrix} \Phi_{11} & \Phi_{12} \\ \Phi_{21} & \Phi_{22} \end{pmatrix} \quad (\text{B1})$$

in the transformed variables is given by

$$\Phi_{11} = \cos(\omega_1 \Delta t_1) \cos(\omega_2 \Delta t_2) - \frac{1}{2} \left(\frac{\omega_1}{\omega_2} + \frac{\omega_2}{\omega_1} \right) \sin(\omega_1 \Delta t_1) \sin(\omega_2 \Delta t_2) \quad (\text{B2})$$

$$\Phi_{12} = \sin(\omega_1 \Delta t_1) \cos(\omega_2 \Delta t_2) + \left(\frac{\omega_1}{\omega_2} \cos^2(\omega_1 \Delta t_1 / 2) - \frac{\omega_2}{\omega_1} \sin^2(\omega_1 \Delta t_1 / 2) \right) \sin(\omega_2 \Delta t_2) \quad (\text{B3})$$

$$\Phi_{21} = -\sin(\omega_1 \Delta t_1) \cos(\omega_2 \Delta t_2) + \left(-\frac{\omega_2}{\omega_1} \cos^2(\omega_1 \Delta t_1 / 2) + \frac{\omega_1}{\omega_2} \sin^2(\omega_1 \Delta t_1 / 2) \right) \sin(\omega_2 \Delta t_2) \quad (\text{B4})$$

$$\Phi_{22} = \Phi_{11}. \quad (\text{B5})$$

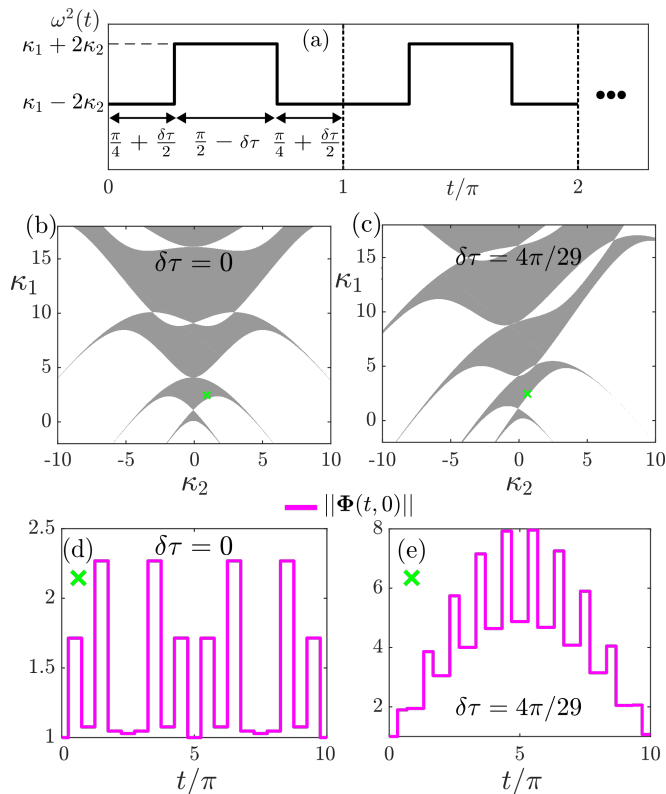


FIG. 10. (a) Piecewise constant frequency $\omega(t)$ of the Meissner oscillator. (b), (c) Stability diagrams for $\delta\tau = 0$ in (b) and $\delta\tau = 4\pi/29$ in (c). (d), (e) Evolution of the norm of the propagator for $\delta\tau = 0$ in (d) and $\delta\tau = 4\pi/29$ in (e). In both panels (d) and (e) we set $\kappa_2 = 0.7585$ and $\kappa_1 = 3\kappa_2$.

In Fig. 10(d) and (e) we present the norm of the propagator matrix $\Phi(t, 0)$ for the same point in the stability chart (green cross) but for the two different $\delta\tau$ used in Fig. 10(b) and (c). In both cases we are in the stable region but transient amplification is observed.

- [1] C. Caloz and Z. L. Deck-Léger, Spacetime Metamaterials—Part I: General Concepts, *IEEE Trans. Antennas Propagat.* **68**, 1569 (2019).
- [2] E. Galiffi et al., Photonics of time-varying media, *Adv. Photonics* **4**, 014002 (2022).
- [3] E. Lustig, O. Segal, S. Saha, C. Fruhling, V. M. Shalaev, A. Boltasseva, and M. Segev, Photonic time-crystals - fundamental concepts, *Optics Express* **31**, 9165 (2023).
- [4] Y. Xiao, D. N. Maywar, and G. P. Agrawal, Reflection and transmission of electromagnetic fields at a temporal boundary, *Opt. Lett.* **39**, 574 (2014).
- [5] E. Lustig, Y. Sharabi, and M. Segev, Topological aspects of photonic time crystals, *Optica* **5**, 1390 (2018).
- [6] S. Yin, E. Galiffi, and A. Alù, Floquet metamaterials, *eLight* **2**, 8 (2022).
- [7] L. Q. Yuan and S. H. Fan, Temporal modulation brings metamaterials into new era, *Light: Sc. Appl.* **11**, 173 (2022).
- [8] M. Lyubarov, Y. Lumer, A. Dikopoltsev, E. Lustig, Y. Sharabi, and M. Segev, Amplified emission and lasing in photonic time crystals, *Science* **377**, 425 (2022).
- [9] D. Torrent, W. J. Parnell, and A. N. Norris, Loss compensation in time-dependent elastic metamaterials, *Phys. Rev. B* **97**, 014105 (2018).
- [10] G. Trainiti, Y. Xia, J. Marconi, G. Cazzulani, A. Erturk, and M. Ruzzene, Time-Periodic Stiffness Modulation in Elastic Metamaterials for Selective Wave Filtering: Theory and Experiment, *Phys. Rev. Lett.* **122**, 124301 (2019).
- [11] J. B. Pendry, E. Galiffi, and P. A. Huidobro, Gain in time dependent media—a new mechanism, *J. Opt. Soc. Am. B* **38**, 3360 (2021).

- [12] L. N. Trefethen, A. E. Trefethen, S. C. Reddy, and T. A. Driscoll, Hydrodynamic stability without eigenvalues, *Science*, **261**, 578 (1993).
- [13] P. J. Schmid, Nonmodal Stability Theory, *Annu. Rev. Fluid Mech.* **39**, 129 (2007).
- [14] B. F. Farrell and P. J. Ioannou, Generalized Stability Theory. Part I: Autonomous Operators, *J. Atmos. Sci.* **53**, 2025 (1996).
- [15] B. F. Farrell and P. J. Ioannou, Generalized Stability Theory. Part II: Nonautonomous Operators, *J. Atmos. Sci.* **53**, 2041 (1996).
- [16] L. N. Trefethen and M. Embree, *Spectra and Pseudospectra*, (Princeton University Press, Princeton, 2005).
- [17] B. Midya, Topological directed amplification, *Phys. Rev. A* **106**, 053513 (2022).
- [18] N. Okuma and M. Sato, Non-Hermitian topological phenomena: A review, *Annu. Rev. Condens. Matter Phys.* **14**, 83 (2023).
- [19] N. Okuma and M. Sato, Hermitian zero modes protected by nonnormality: Application of pseudospectra, *Phys. Rev. B* **102**, 014203 (2020).
- [20] Y. O. Nakai, N. Okuma, D. Nakamura, K. Shimomura, and M. Sato, Topological enhancement of non-normality in non-Hermitian skin effects, arXiv:2304.06689 (2023).
- [21] D. Holberg and K. Kunz, Parametric Properties of Fields in a Slab of Time-Varying Permittivity, *IEEE Trans. Antennas Propag.* **14**, 183 (1966).
- [22] T. T. Koutserimpas, A. Alù, and R. Fleury, Parametric amplification and bidirectional invisibility in \mathcal{PT} -symmetric time-Floquet systems, *Phys. Rev. A* **97**, 013839 (2018).
- [23] P. J. Schmid, and D. S. Henningson, *Stability and Transition in Shear Flows*, (Springer, New York, 2001).
- [24] N. W. McLachlan, *Theory and Application of Mathieu Functions*, (Dover, New York, 1964).
- [25] L. Ruby, Applications of the Mathieu equation, *Am. J. Phys.* **64**, 39 (1996).
- [26] M. Bukov, L. D'Alessio and A. Polkovnikov, Universal high-frequency behavior of periodically driven systems: from dynamical stabilization to Floquet engineering, *Adv. Phys.* **64**, 139 (2015)
- [27] W. Paul, Electromagnetic traps for charged and neutral particles, *Rev. Mod. Phys.* **62**, 531 (1990).
- [28] T. B. Benjamin and F. Ursell, The stability of the plane free surface of a liquid in vertical periodic motion, *Proc. Roy. Soc. London, Ser. A* **225**, 505 (1954).
- [29] M. Abramowitz and I. A. Stegun, *Handbook of Mathematical Functions*, (Dover, New York, 1972).
- [30] L. Brillouin, *Wave Propagation in Periodic Structures*, (McGraw-Hill, New York, 1946).
- [31] A. H. Nayfeh, *Introduction to Perturbation Techniques* (Wiley, New York, 1993).
- [32] C. Bender and S. Orszag, *Advanced Mathematical Methods for Scientists and Engineers I* (Springer, New York, 1999).
- [33] G. Teschl, *Ordinary differential equations and dynamical systems*, (American Mathematical Soc., 2012).
- [34] D. Jordan and P. Smith, *Nonlinear Ordinary Differential Equations: An Introduction for Scientists and Engineers* (Oxford University Press, Oxford, 2007).
- [35] A. A. Grandi, S. Protière, A. Lazarus, Enhancing and controlling parametric instabilities in mechanical systems, *Extreme Mechanics Letters* **43** 101195 (2021).
- [36] T. T. Koutserimpas and R. Fleury, Electromagnetic waves in a time periodic medium with step-varying refractive index, *IEEE Trans. Antennas Propag.* **66**, 5300 (2018).
- [37] Note that the linearization of a nonlinear dynamical system around a periodic solution leads in many cases to Hill's differential equation (for instance the linearization of the Duffing equation leads to Mathieu equation), suggesting a connection between nonlinear evolution and transient amplification.
- [38] K. Yu Bliokh, Generalized geometric phase of a classical oscillator, *J. Phys. A: Math. Gen.* **36**, 1705 (2003).
- [39] Notice that the variables X and Y are real only when the parameter $\omega^2(t)$ is positive, that is inside the cone $\delta = 2|q|$ that is shown in Fig. 1(a). At the boundary of this cone as well as at the outside region, $\omega(t)$ becomes zero within each period π , suggesting that the variable Y acquires singularities. As a result, another suitable transformation should be considered that describes the amplification features correctly in this region. However, there is no reason for the amplification features to be qualitatively different between these two regions, since the initial variables f and \dot{f} which express the physical properties of the system change smoothly across the whole stability chart. Therefore, we restrict our analysis only at the region that locates inside the cone $\delta = 2|q|$, where the norm of the vector $\xi(t)$ quantifies properly the amplification features.
- [40] G. W. Steward, On the early history of the singular value decomposition, *SIAM Rev.* **35**, 551 (1993).
- [41] T. Mitchell, Computing the Kreiss constant of a matrix, *SIAM J. Matrix Anal. Appl.*, **41**, 1944 (2020).
- [42] Here we are considering a case where the propagator is periodic and its maximum is taken over one period. We have tried also cases of non-periodic evolution over very long time and we were unable to see different behavior from the one described.
- [43] M. V. Berry, Mode degeneracies and the Petermann excess-noise factor for unstable lasers, *J. Mod. Opt.* **50**, 63 (2003).
- [44] S.-Y. Lee, Decaying and growing eigenmodes in open quantum systems: Biorthogonality and the Petermann factor, *Phys. Rev. A* **80**, 042104 (2009).
- [45] We shall make the following remarks regarding the intervals that the two times t and t_0 must scan in order to get the desired maximum numerically: First, even though the quantity $\omega(t)$ is periodic with period π , it is sufficient for the time t_0 to scan the interval $[0, \pi/2]$ (see Fig. 6). Second, when the exponent γ is a rational number it is sufficient for t to scan the interval $[0, \pi m_2]$ (recall Fig. 3) in order to reach the maximum amplification.